Maximum Ratio Transmission for Space-Polarization Division Multiple Access in Dual-Polarized MIMO System

Jun-Ki Hong[1], Han-Shin Jo[2], Cheol Mun[3], and Jong-Gwan Yook[1]
[1]Dept. of Electrical and Electronic Engineering, Yonsei University
Seoul, 120-749, Korea
[e-mail: junki_hong, jgyook@yonsei.ac.kr]
[2]Dept. of Electronics and Control Engineering, Hanbat National University
Daejeon, 305-719, Korea
[e-mail: hsjo@hanbat.ac.kr]
[3]Dept. of Information and Communication Engineering, Korea National University of Transportation
Chungju, 380-702, Korea
[e-mail: chmun@ut.ac.kr]
*Corresponding author: Jong-Gwan Yook

Received March 6, 2015; revised August 3, 2015; accepted August 19, 2015; published August 31, 2015

Abstract

The phenomena of higher channel cross polarization discrimination (XPD) is mainly observed for future wireless technologies such as small cell network and massive multiple-input multiple-output (MIMO) system. Therefore, utilization of high XPD is very important and space-polarization division multiple access (SPDMA) with dual-polarized MIMO system could be a suitable solution to high-speed transmission in high XPD environment as well as reduction of array size at base station (BS). By SPDMA with dual-polarized MIMO system, two parallel data signals can be transmitted by both vertically and horizontally polarized antennas to serve different mobile stations (MSs) simultaneously compare to conventional space division multiple access (SDMA) with single-polarized MIMO system. This paper analyzes the performance of SPDMA for maximum ratio transmission (MRT) in time division duplexing (TDD) system by proposed dual-polarized MIMO spatial channel model (SCM) compare to conventional SDMA. Simulation results indicate that how SPDMA utilizes the high XPD as the number of MS increases and SPDMA performs very close to conventional SDMA for same number of antenna elements but half size of the array at BS.

Keywords: Space-polarization division multiple access (SPDMA), Cross polarization discrimination (XPD), Dual-polarized antenna, Maximum ratio transmission (MRT), Time division duplexing (TDD)

A preliminary version of this paper was presented at ICONI 2014, and was selected as an outstanding paper.
This research was supported by the MSIP(Ministry of Science, ICT and Future Planning), Korea, under the C-ITRC(Convergence Information Technology Research Center) (IITP-2015-H8601-15-1008) supervised by the IITP(Institute for Information & communications Technology Promotion) and by the MSIP(Ministry of Science, ICT and Future Planning), Korea, under the Global IT Talent support program (IITP-2015-ITAH090414011002000100010100) supervised by the IITP(Institute for Information and Communication Technology Promotion)"

http://dx.doi.org/10.3837/tiis.2015.08.0017 **ISSN : 1976-7277**

1. Introduction

In recent years, the data traffic increases mainly driven by the popularity of various smart devices with heavy data usage such as internet access and video streaming services. To handle these tremendous mobile data traffic, two major 5G technologies are currently being intensely investigated: small cell and massive multiple-input multiple-output (MIMO) system. Small cell increases the system capacity by decreasing cell sizes to increase the number of line-of-sight (LOS) between transmitter (Tx) and receiver (Rx). Another key technology is massive MIMO system. Massive MIMO system comprises hundreds of antenna elements that create the sharp beams and increase the transmit diversity at Tx. Therefore, channel characteristics of both small cell and massive MIMO system are found to have high cross polarization discrimination (XPD) with lower angular spread (AS) [1] and its channel statistics over the array is changed due to its large size of the array [1],[2].

Polarization division multiple access (PDMA) using dual-polarized antennas in high XPD could increase data rate by almost double via vertically and horizontally polarized channels. Consequently, the physical array size of the PDMA with dual-polarized MIMO system can be cut in half while dual-polarized antenna supports the same degree of freedom compared to two spatially separated the single-polarized antennas. However, polarization mismatch is occurred by the random handset orientation where the use of conventional single-polarized antenna receiving the signal by only one polarization results in the power loss at the Rx. The upper bound of capacity loss due to polarization mismatch is known to be 2 bit/s/Hz [3]. To minimize capacity loss by polarization mismatch, dual-polarized antenna should be equipped at a Rx to receive signals by both vertically and horizontally polarized antennas. Therefore, it is clear that dual-polarized antenna can be the potential antenna structure for future massive MIMO system to overcome limitation of physical array size and polarization mismatching.

The several dual-polarized MIMO channel models have been proposed in previous literatures. Performance evaluation of dual-polarized MIMO system with 3rd generation partnership project (3GPP) dual-polarized MIMO channel is achieved through mixed vertically and horizontally polarized signals at mobile station (MS) [4]. The polarization diversity under Rayleigh fading environment is analyzed in [5]. The performance analysis of PDMA with polarization filtering detection is achieved where two data signals are transmitted via vertically and horizontally polarized antenna elements to different MSs at the same time [6]. However, previous PDMA technique is lack of spatial diversity at BS since only one dual-polarized antenna is installed at BS.

Afterwards, more advanced space-polarization division multiple access (SPDMA) for dual-polarized frequency division duplexing (FDD) MIMO system is introduced in [7]. The SPDMA is an extension technique of space division multiple access (SDMA) which achieves the diversity gains not only by spatial domain but also by polarization domain. This paper concludes that SPDMA outperforms conventional SDMA for the same size of array when MS fully exploiting the multiple access in both space and polarization domains.

Previously dual-polarized MIMO channel is suggested based on Ricean fading channel to evaluate performance of SPDMA in [7]. However, the realistic geometry parameters such as AS, path delay, and antenna gains would be required to evaluate the practical performance of SPDMA. Hence, geometry-based dual-polarized MIMO spatial channel model (SCM) is proposed to evaluate practical performance of SPDMA. To the best of our knowledge, this is the first study that addresses the practical performance of SPDMA through dual-polarized

MIMO SCM in TDD system.

The rest of the paper is organized as follows. In section 2, description of the proposed dual-polarized SCM is presented. In section 3, SPDMA and its multi-MS scheduling algorithm are described. In section 4, performance evaluation of SPDMA is achieved compare to SDMA via two simulation scenarios; same number of antenna elements and identical array size of SDMA. Finally, section 5 summarizes the key simulation results and future extension.

2. Dual-Polarized MIMO SCM

2.1 Fundamental Concept of Proposed Dual-polarized MIMO SCM

To analyze the performance of SPDMA by downlink system-level simulation, the dual-polarized MIMO channel coefficient is proposed which considers independent vertical to vertical (VV), horizontal to vertical (VH), vertical to horizontal (HV), and horizontal to horizontal (HH) channel polarizations between a dual-polarized Tx and Rx.

The proposed dual-polarized MIMO SCM consists of $S/2$ co-located dual-polarized antennas (total S antenna elements) at base station (BS) and $U/2$ co-located dual-polarized antennas (total U antenna elements) at MS. Then, downlink received signal of the kth MS can be written as

$$y_k = \mathbf{H}_k \mathbf{x} + \mathbf{z}_k \tag{1}$$

where $\mathbf{H}_k$ denotes the $U \times S$ dual-polarized MIMO channel matrix of the kth MS, $\mathbf{x}$ is $U \times 1$ transmitted signal vector with power constraint $\varepsilon[\|x\|^2] \leq \mathrm{P}$, and $\mathbf{z}_k$ denotes the $U \times 1$ additive complex Gaussian noise at MS. The channel configuration of 2×2 dual-polarized MIMO at kth MS, $\mathbf{H}_k$, is presented in **Fig. 1** as the simplest example.

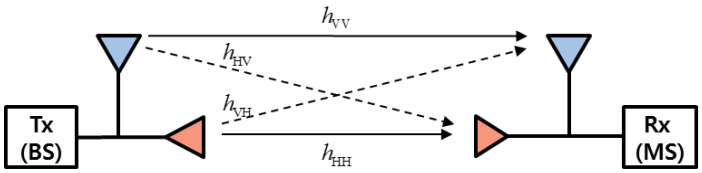

Fig. 1. 2×2 dual-polarized MIMO channel

Basically, 2×2 matrix consists of four independent propagation channels between dual-polarized Tx and Rx antennas can be represented by

$$\mathbf{H} = \begin{bmatrix} h_{VV} & h_{HV} \\ h_{VH} & h_{HH} \end{bmatrix} \tag{2}$$

where each element is defined as follows.

h_{VV}: vertical transmit and vertical receive polarization

h_{HV}: vertical transmit and horizontal receive polarization

h_{VH}: horizontal transmit and vertical receive polarization

h_{HH}: horizontal transmit and horizontal receive polarization

2.2 Dual-polarized MIMO SCM

The proposed dual-polarized MIMO SCM is a geometry-based channel model that describes multipath directions of the arrival and departure angles, path delays, AS, and antenna gains between BS and MS.

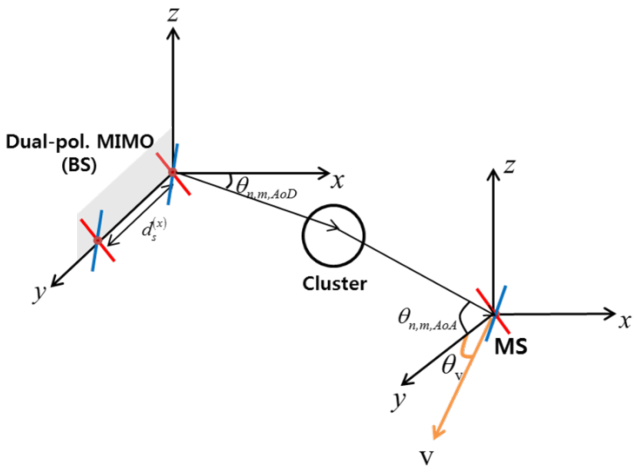

Fig. 2. Geometries and parameters of the proposed dual-polarized MIMO SCM

As shown in **Fig. 2**, BS and MS are equipped with ±45˚slanted dual-polarized antennas. BS is consists of spatially separated dual-polarized antennas and equispaced at interval of $d_s^{(x)}$ on *x*-axis.

The channel matrix of proposed dual-polarized MIMO SCM is composed by *U*/2 co-located dual-polarized transmitting antennas (*U* total antenna elements) at BS and *S*/2 co-located dual-polarized receiving antennas (*S* total antenna elements) at MS. Then, (*u*,*s*)th dual-polarized MIMO channel composed of *n*th multipath (*n* = 1,…, *N*) and each of the *N* multipath component is comprised of *M* subpaths. Proposed dual-polarized MIMO channel is generated by *N*=6 and *M*=20 which is recommended by 3GPP [8]. The proposed dual-polarized MIMO channel between BS and MS at time *t* can be represented by $\mathrm{H}_{u,s,n}(t)$ as equation (3)

$$\mathbf{H}_{u,s,n}(t)=\sqrt{\frac{P_n\sigma_{SF}}{M}}\sum_{m=1}^{M}\left(\begin{bmatrix}\mathrm{VV} & \mathrm{HV}\\ \mathrm{VH} & \mathrm{HH}\end{bmatrix}\times\exp\left(\beta_{AoD}\right)\times\exp\left(\beta_{AoA}\right)\times\exp\left(\psi_{AoA}\right)\times t\right) \quad (3)$$

where

$$\mathrm{VV}=\chi_{BS,V}\left(\theta_{n,m,AoD}\right)\left(\sqrt{\frac{\mathrm{XPD}}{1+\mathrm{XPD}}}\exp\left(j\Phi_{n,m}^{(v,v)}\right)\right)\chi_{MS,V}\left(\theta_{n,m,AoA}\right)$$

$$\mathrm{HV}=\chi_{BS,V}\left(\theta_{n,m,AoD}\right)\left(\sqrt{\frac{1}{1+\mathrm{XPD}}}\exp\left(j\Phi_{n,m}^{(h,v)}\right)\right)\chi_{MS,H}\left(\theta_{n,m,AoA}\right)$$

$$\mathrm{VH} = \chi_{BS,H}\left(\theta_{n,m,AoD}\right)\left(\sqrt{\frac{1}{1+\mathrm{XPD}}}\exp(j\Phi_{n,m}^{(v,h)})\right)\chi_{MS,V}\left(\theta_{n,m,AoA}\right)$$

$$\mathrm{HH} = \chi_{BS,H}\left(\theta_{n,m,AoD}\right)\left(\sqrt{\frac{\mathrm{XPD}}{1+\mathrm{XPD}}}\exp(j\Phi_{n,m}^{(h,h)})\right)\chi_{MS,H}\left(\theta_{n,m,AoA}\right)$$

$$\beta_{AoD} = j2\pi\lambda^{-1}\left\{(u_x - 1)d_s^{(x)}\cos\left(\theta_{n,m,AoD}\right)\right\}$$

$$\beta_{AoA} = j2\pi\lambda^{-1}\left\{(s_x - 1)d_u^{(x)}\cos\left(\theta_{n,m,AoA}\right)\right\}$$

$$\psi_{AoA} = j2\pi\lambda^{-1}\|\mathrm{v}\|\left[\cos\left(\theta_{n,m,AoA} - \theta_{\mathrm{v}}\right)\right]$$

where VV, HV, VH, and HH represent independent propagation channels between dual-polarized Tx and Rx as shown as Fig. 1. Moreover, β_{AoD} and β_{AoA} denote angle phase due to BS and MS respectively. Ψ_{AoA} represents Doppler shift term at MS and notations are listed in **Table 1**.

Table 1. Dual-polarized MIMO SCM notations

P_n	The power of the *n*th path
σ_{SF}	The lognormal shadow fading
M	The number of subpaths per path
$\theta_{n,m,AoD}$	Angle of departure (AoD) for the *m*th subpath of the *n*th path at the BS with respect to the BS broadside
$\theta_{n,m,AoA}$	Angle of arrival (AoA) for the *m*th subpath of the *n*th path at the MS with respect to the MS broadside
$\chi_{BS,V}$	BS antenna complex response for the V-pol. component
$\chi_{BS,H}$	BS antenna complex response for the H-pol. component
$\chi_{MS,V}$	MS antenna complex response for the V-pol. component
$\chi_{MS,H}$	MS antenna complex response for the H-pol. component
$\Phi_{n,m}^{(x,y)}$	The random phase shift between V(or H) of the BS and V(or H) component of MS for the *m*th subpath
$\|\mathbf{v}\|$	The magnitude of the MS velocity (**v**) vector
θ_{V}	The azimuth angle of the MS velocity vector
j	Square root of -1
$d_s^{(x)}$	The distance in meters between BS antenna element *s* and the reference (*s*=1) antenna element where d_1= 0.

The first matrix of equation (3) represents independent VV, VH, HV, and HH propagation channels between Tx and Rx including XPD. XPD represents the ratio of the co-polarized to the cross-polarized average power at a Rx as follows

$$\begin{aligned}\mathrm{XPD} &= \frac{\text{Co-polarized Rx power}}{\text{Cross-polarized Rx power}} \\ &= \frac{\mathrm{E}\left\{|h_{VV}|^2\right\}}{\mathrm{E}\left\{|h_{VH}|^2\right\}} = \frac{\mathrm{E}\left\{|h_{HH}|^2\right\}}{\mathrm{E}\left\{|h_{HV}|^2\right\}}\end{aligned} \tag{4}$$

where XPD quantifies the extent of the polarization mismatching and simulation results in section 4 show how XPD values affect the performance of proposed MIMO systems.

The proposed channel matrix notation is indicated by the number of Rx×Tx antenna elements. Consequently, 2×2 dual-polarized MIMO channel can be extended to 2×4 dual-polarized MIMO channel by adding another 2×2 dual-polarized channel beside reference 2×2 dual-polarized MIMO channel matrix. For example, 2×4 dual-polarized MIMO SCM represents two spatially separated dual-polarized antennas at BS and one dual-polarized antenna at MS. Then, 2×4 dual-polarized MIMO channel matrix can be expressed as

$$\mathbf{H}_{2\times 4,dual-pol.}=\begin{bmatrix} h_{11,VV} & h_{12,HV} & h_{13,VV} & h_{14,VH} \\ h_{21,VH} & h_{22,HH} & h_{23,HV} & h_{24,HH} \end{bmatrix} \tag{5}$$

where h_{u,s,P_u,P_s} denotes the propagation channels from the sth Tx antenna element with P_s polarization to the uth Rx antenna element with P_u polarization. Furthermore, the first and second column indexes (s=1 and 2) represent the first co-located dual-polarized antenna and the third and fourth column indexes (s=3 and 4) represent the second co-located dual-polarized antenna at BS.

2.3 Single-polarized MIMO SCM

Proposed single-polarized MIMO channel matrix can be represented by vertical single-polarized antennas at BS and one co-located dual-polarized antenna at MS. Thus, the channel coefficients are simply obtained by extracting the odd column indexes from the proposed dual-polarized MIMO channel matrix. For instance, 2×4 single-polarized MIMO channel matrix, $\mathrm{H}_{2\times 4,single-pol.}$, can be expressed by vertical single-polarized antenna terms from 2×8 channel matrix, $\mathrm{H}_{2\times 8,dual-pol.}$, as follows

$$\mathbf{H}_{2\times 4,single-pol.}=\begin{bmatrix} h_{11,VV} & h_{13,VV} & h_{15,VV} & h_{17,VV} \\ h_{21,HV} & h_{23,HV} & h_{25,HV} & h_{27,HV} \end{bmatrix}. \tag{6}$$

Similarly, 2×2 single-polarized MIMO channel matrix can be written by two odd column indexes as follows

$$\mathbf{H}_{2\times 2,single-pol.}=\begin{bmatrix} h_{11,VV} & h_{13,VV} \\ h_{21,HV} & h_{23,HV} \end{bmatrix}. \tag{7}$$

In Section 4, the performance of SPDMA and SDMA are evaluated by proposed dual- and single-polarized MIMO SCMs respectively.

3. MRT-based SPDMA

3.1 SPDMA vs SDMA

The concept of conventional SDMA is utilization of spatial domain by spatial multiplexing and this technique makes it possible to increase the performance by serving different MSs simultaneously in spatial domain. Afterwards, SPDMA and its codebook are proposed for

dual-polarized MIMO system in [7]. As mentioned before, SPDMA is the extended technique of SDMA with extra polarization utilization while SDMA serves signals in spatial domain only. Since MRT transmit signals by along the strongest eigenmode at BS and transmitted signals are combined by maximal ratio combing at MS, SPDMA enables to maximize the performance for high XPD by transmitting two different data signals via two orthogonally polarized propagation channels.

Fig. 3 (a) and (b) represent the basic idea of signal transmission of SPDMA and SDMA respectively.

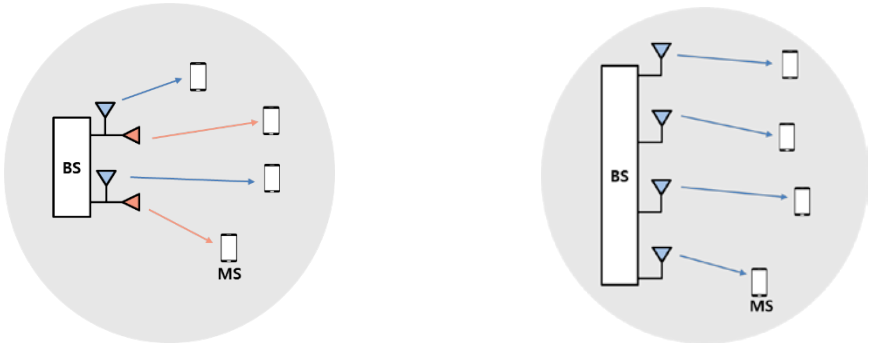

(a) (b)

Fig. 3. Transmit configuration of (a) SPDMA and (b) SDMA

As shown as **Fig. 3** (a), two signals can be transmitted by one co-located dual-polarized antenna since SPDMA utilizes not only by space domain but also by polarization domain. Therefore, dual-polarized MIMO system with SPDMA able to achieve same degrees of freedom by the same number of antenna elements but half array size compare to spatially separated single-polarized MIMO system with SDMA.

3.2 Proposed Multi-MS Scheduling Algorithm

The data symbols for the selected S MSs from total K MSs are linearly precoded by maximum ratio transmission (MRT) and transmitted signal vector can be represented as follows

$$\mathbf{x} = \mathbf{F}\mathbf{b} = \sum_{k=1}^{S} \mathbf{f}_k b_k \tag{8}$$

where $\mathbf{F} = [\mathbf{f}_1\ \mathbf{f}_2 \cdots \mathbf{f}_S]$ is the $S\times S$ precoding matrix where $\mathbf{f}_k$ is the $S\times 1$ precoding vector for the kth MS among selected S MSs and $\mathbf{b} = [b_1\ b_2 \cdots b_S]^T$ is the $S\times 1$ transmit symbol vector where b_k is the transmit symbol for the kth MS among the selected S MSs.

Then achievable rate of the kth MS by MMSE receiver can be written as

$$C_k = \log_2\left(1 + b_k^* \mathbf{f}_k^{\mathrm{H}} \mathbf{H}_k^{\mathrm{H}} \left(\mathbf{I} + \sum_{l=1, l\neq k}^{S} \mathbf{H}_k \mathbf{f}_l b_l b_l^* \mathbf{f}_l^{\mathrm{H}} \mathbf{H}_k^{\mathrm{H}}\right)^{-1} \mathbf{H}_k \mathbf{f}_k b_k\right) \tag{9}$$

where $\mathbf{H}_k$ denotes $U\times S$ dual-polarized MIMO channel of the kth MS and $\mathbf{I}$ represents $S\times S$ identity matrix respectively. The precoding vector of MRT of the kth MS is denoted by $\mathbf{f}_k$ obtained as

$$\mathbf{f}_k = \mathbf{V}_k, \tag{10}$$

$$\mathrm{SVD}\left[\mathbf{H}_k\right] = \mathbf{U}_k \mathbf{\Sigma}_k \mathbf{V}_k^{\mathrm{H}}, \tag{11}$$

where SVD represents the singular value decomposition. $\mathbf{U}_k$, $\mathbf{\Sigma}_k$, and $\mathbf{V}_k$ represent $S \times S$ complex unitary matrix, $S \times U$ rectangular diagonal matrix, and $U \times U$ complex unitary matrix of the kth MS, respectively.

To evaluate the performance of proposed simulation scenarios, multi-MS selection algorithm is proposed to achieve the maximum throughput with optimal MS selections in the sector. The proposed MS selection algorithm is specified as follows.

Algorithm 1: MS Selection Algorithm

initialize $G_{opt.} = \{\varnothing\}$, $C_{max} = 0$, $a = 0$

do

$$n = \arg\max_{n \in O, n \neq G_{opt.}} \frac{\sum_{k \in \{n, G_{opt.}\}} \log_2\left(1 + \gamma_k(t)\right)}{\bar{\gamma}_k(t)}$$

$$C = \sum_{k \in \{n, G_{opt.}\}} \log_2\left(1 + \gamma_k(t)\right)$$

if $C > C_{max.}$

$G_{opt.} = \{G_{opt.}, n\}$

$R_{max} = R$

$a = 1$

end

while $a = 1$ **and** $|G_{opt.}| < S_{tx}$

where γ_k denotes SINR and $\bar{\gamma}_k$ represents historical average SINR of kth MS to achieve proportional fair scheduling which avoids starvation for MS on bad channel conditions [8]. O represents the universal set of MSs. S_{tx}, C, and C_{max} represent the number of Tx antenna elements, throughput, and the maximum throughput of the kth MS, respectively.

According to proposed Algorithm 1, the throughput is obtained by add a MS candidate in subset $G_{opt.}$ until the maximum throughput is achieved. The proposed MS selection algorithm is applied to obtain the maximum sector throughput from simulation scenarios with optimal MS selections.

3.3 TDD Operations

In traditional FDD systems, channel state information (CSI) is estimated by training pilot symbols at Rx and sent to Tx through the feedback channel. Since the pilot symbols for each transmit antenna is allocated to different time or frequency resource for the exact estimation of CSI, the FDD system with the very large number of antennas is not affordable for CSI estimation due to its dramatically increased CSI information and result in requirement of extremely large amount of radio resources. On the other hand, time division duplexing (TDD) would be more reliable technique to estimate CSI of massive MIMO system where training signal is not required and alternatively requires the channel reciprocity between forward and

reverse channels. Thus, the perfect CSI and TDD system is assumed to evaluate proposed dual-polarized MIMO system with SPDMA technique.

4. Performance evaluation

4.1 Simulation Scenarios

To analyze the performance of SPDMA with dual-polarized MIMO system, the sector throughput of 4Tx/2Rx SPDMA, 4Tx/2Rx and 2Tx/2Rx SDMA are evaluated as shown in **Fig. 4**. 4Tx/2Rx and 2Tx/2Rx SDMA represent the same number of antenna elements and identical array size as proposed 4Tx/2Rx SPDMA. Furthermore, the sector throughput of 8Tx/2Rx SPDMA, 8Tx/2Rx SDMA, and 4Tx/2Rx SDMA are evaluated to investigate the effect of increased number of antenna elements at BS.

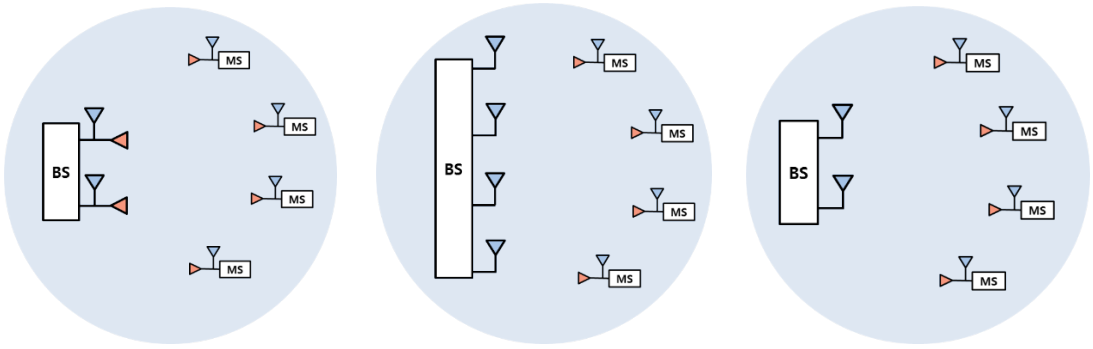

(a) (b) (c)

Fig. 4. Simulation scenarios of (a) 4Tx/2Rx SPDMA, (b) 4Tx/2Rx SDMA, and (c) 2Tx/2Rx SDMA

Aforementioned, each MS consists of one dual-polarized antenna since MMSE receiver able to decide whether MS receives one strongest signal or two combined signals after SINR calculations. Then proposed MS selection algorithm will determine best MS combinations to achieve maximum throughputs in sector. For instance, some MS will prefer to receive one strongest signals and the other MSs will prefer to receive two signals depend on channel conditions at the same time. Furthermore, MS is assumed as one co-located dual-polarized antenna for all simulation scenarios to achieve fair comparison of the performances.

Important simulation parameters are shown in **Table 2**. Simulation scenarios of urban macro are adapted by 3GPP [9] and evaluation of proposed simulation models are followed by [10].

Table 2. Simulation parameters

Parameter	Assumption
Cellular layout	Hexagonal grid, 19 sites, and 3 sectors per site [10]
Simulation scenarios	Urban macro with AS 8˚ and 15˚ [9]
Sector radius	350 m
Carrier frequency	2.9 GHz
System bandwidth	10 MHz
Channel estimation	Ideal
XPD	0, 10, and 20 dB
Tx height	35 m
Rx height	1.5 m
Antenna spacing	0.5λ

Tx transmit power	43 dBm
Detection algorithm	MMSE
Speed of moving Rx	3 km/h
Noise figure	7 dB
Pathloss	COST 231 Hata model [11]
Simulation scenarios 1	4Tx/2Rx SPDMA, 4Tx/2Rx SDMA, and 2Tx/2Rx SDMA
Simulation scenarios 2	8Tx/2Rx SPDMA, 8Tx/2Rx SDMA, and 4Tx/2Rx SDMA

4.2 Simulation Results

In this subsection, the comparative simulation results of proposed systems are presented. **Fig. 5** and **Fig. 6** show the sector throughput of 4Tx/2Rx SPDMA, 2Tx/2Rx SDMA, and 4Tx/2Rx SDMA of AS 8˚ and 15˚ respectively as a function of the number of MSs.

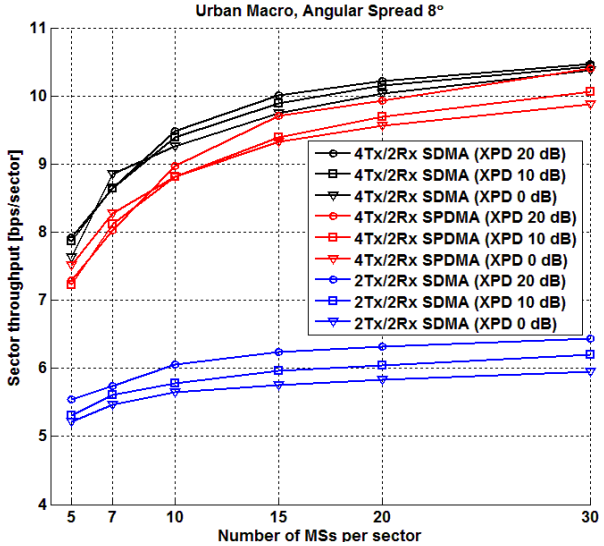

Fig. 5. Throughput comparison of 4Tx/2Rx SDMA, 4Tx/2Rx SPDMA, and 2Tx/2Rx SDMA for urban macro with AS 8˚

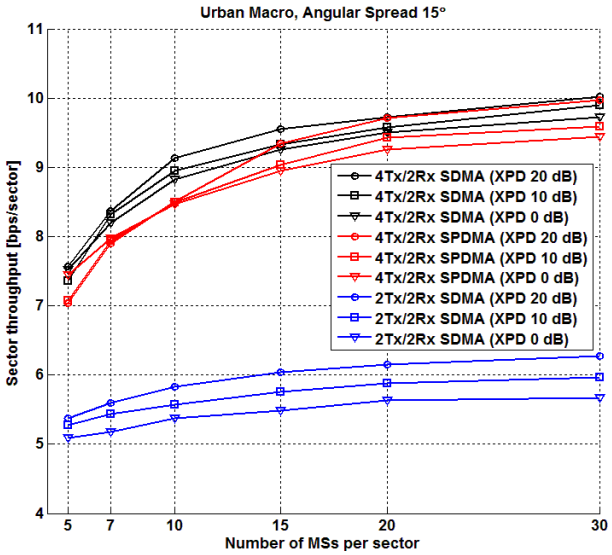

Fig. 6. Throughput comparison of 4Tx/2Rx SDMA, 4Tx/2Rx SPDMA, and 2Tx/2Rx SDMA for urban macro with AS 15˚

As shown in **Fig. 5** and **Fig. 6**, the sector throughput of 4Tx/2Rx SDMA is always slightly higher than that of 4Tx/2Rx SPDMA for every simulation results due to its less interferences between antenna elements. Nevertheless, it is notable that the proposed 4Tx/2Rx SPDMA performs very close to conventional 4Tx/2Rx SDMA by half-size array and has almost 1.6 times higher throughput gain over 2Tx/2Rx SDMA for identical array size. This is remarkable simulation results since the physical size of antenna arrays is a major obstacle to implement BS with a large number of antennas.

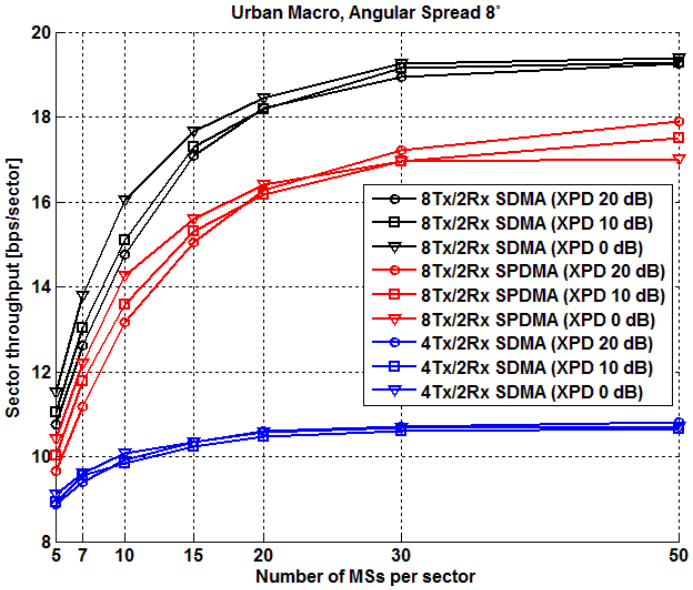

Fig. 7. Throughput comparison of 8Tx/2Rx SPDMA, 8Tx/2Rx SDMA, and 4Tx/2Rx SDMA for urban macro with AS 8˚

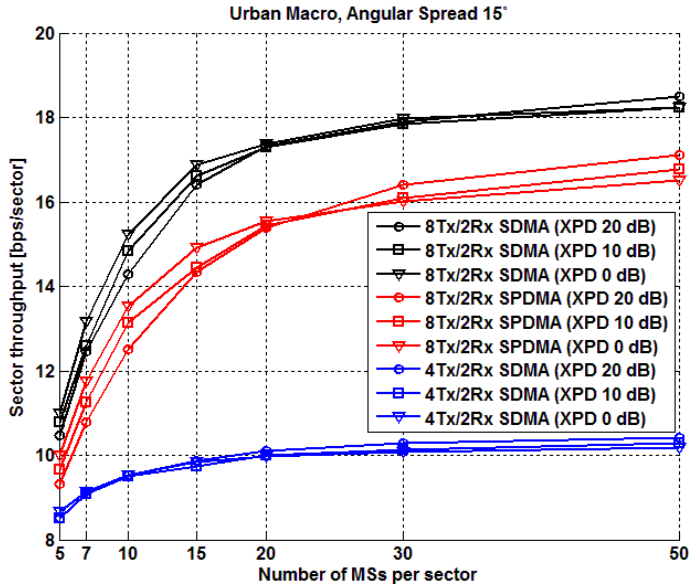

Fig. 8. Throughput comparison of 8Tx/2Rx SPDMA, 8Tx/2Rx SDMA, and 4Tx/2Rx SDMA for urban macro with AS 15˚

Fig. 7 and **Fig. 8** show the sector throughput of 8Tx/2Rx SPDMA, 8Tx/2Rx SDMA, and 4Tx/2Rx SDMA of AS 8˚ and 15˚ respectively as a function of number of MS. As shown as **Fig. 7** and **Fig. 8**, 8Tx/2Rx SDMA outperforms 8Tx/2Rx SPDMA with wider throughput gaps compared to simulation result of 4Tx/2Rx SPDMA and 4Tx/2Rx SDMA. This is because more interference arises between co-located two orthogonal antennas for larger dual-polarized antenna array. However, 8Tx/2Rx SPDMA outperforms 1.6 higher than 8Tx/2Rx SDMA. Furthermore, as shown in **Fig. 5~8,** the overall sector throughput of urban macro with AS 8˚ outperforms urban macro with AS 15˚ because of lower level of intra-stream interference are generated for lower angle of AS.

Additionally, simulation results from **Fig. 5~8** show that sector throughput is significantly dependent on the level of XPD which affects level of antenna correlations and interference between vertically and horizontally polarized antennas at MS. The sector throughput is higher for lower XPD value when small number of MSs are existed in sector since each MS prefers to receive two uncorrelated signals simultaneously instead of receiving highly correlated two signals simultaneously. This is because lower XPD leads lower antenna correlation and interferences between vertically and horizontally polarized antennas at MS but higher XPD leads higher antenna correlation and interferences between two orthogonally polarized antennas. Therefore, each MS prefers to receive two different signals with lower correlation and interferences when small number of MSs are exist in sector.

On the other hand, sector throughput is increased for higher value of XPD as the number of MSs are increased in sector. This is because dual-polarized antennas at BS prefer to transmit two independent signals to different MSs simultaneously with high directivity (high XPD) since large number of MSs increase the probability of find MS with high directivity among MS candidates in sector. In other words, dual-polarized antenna at MS prefer to select and receive only one strongest signal with high directivity instead of receiving two signals since intra-interferences occurs when two signals are received by MS.

5. Conclusions

In this paper, SPDMA with MRT for dual-polarized MIMO system is proposed. The comparative study are conducted on SDMA and SPDMA by dual- and single-polarized MIMO systems respectively.

Simulation results show that how XPD values affect the performances of SPDMA and SDMA as the number of MS are increased. SPDMA with dual-polarized antenna MIMO system outperforms almost 1.6 times higher than SDMA with single-polarized MIMO system for identical array size. This simulation results indicate that dual-polarized MIMO system with SPDMA could be the key technology to utilize XPD and array size of massive MIMO system could be reduced by half compare to conventional single-polarized MIMO system with SDMA.

References

[1] J-U. Jeong, J-H. Kim, and C. Mun, “Analysis of massive MIMO wireless channel characteristics,” *J. of The Korean Inst. of Commun. and Inform. Sci.*, vol. 38B, no. 03, pp. 216–221, Mar. 2013.

[2] X. Gao, F. Tufvesson, O. Edfors, and F. Rusek, "Massive MIMO channels - Measurements and models," *Signals, Systems and Computers*, 2013 Asilomar Conference, vol., no., pp.280, 284, 3-6 Nov. 2013. Article (CrossRef Link)

[3] H. Joung, H-S. Jo, C. Mun, and J-G. Yook, "Capacity loss due to polarization-mismatch and

space-correlation on MISO channel," *IEEE Transactions on Wireless Communications*, vol. 13, no. 4, pp. 2124-2136, Apr. 2014. Article (CrossRef Link)

[4] Q.Wang, C. Hou, Y. Lu, Z. Yan, and N. Liu, "Performance evaluation of polarization diversity and space diversity under 3GPP channel model," in *Proc. of Proceedings of the 2008 international conference on advanced infocomm technology*, ACM, New York, NY, USA, Article 46. July. 2008. Article (CrossRef Link)

[5] R. U. Nabar, H. Bolcskei, V. Erceg, D. Gesbert, and A. J. Paulraj, "Performance of multiantenna signaling techniques in the presence of polarization diversity," *IEEE Transactions on signal processing*, vol. 50, no. 10, pp. 2553-2562, Oct. 2002. Article (CrossRef Link)

[6] S-C. Kwon, G.L. Stuber, "Polarization Division Multiple Access on NLoS Wide-Band Wireless Fading Channels," *IEEE Transactions on Wireless Communications*, vol.13, no.7, pp.3726-3737, July 2014. Article (CrossRef Link)

[7] H. Joung, H-S. Jo, C. Mun, and J-G. Yook, "Space-polarization division multiple access system with limited feedback," *KSII Transactions on Internet and Information Systems*, vol. 8, no. 4, pp. 1292-1306, Apr. 2014. Article (CrossRef Link)

[8] V. Lau, "Proportional fair spatial scheduling for wireless access point with multiple antenna - reverse link with scalar feedback", *Proc. IEEE GLOBECOM'02*, 2002, pp. 763-767. Article (CrossRef Link)

[9] "Spatial channel model for Multiple Input Multiple Output (MIMO) simulations," 3GPP TR 25.996, 12.0.0 ed., 2014.

[10] R. Srinivasan, ed., "IEEE 802.16m Evaluation Methodology Document (EMD), IEEE 802.16m-Advanced Air Interface," Jan. 2009.

[11] COST Action 231, "Digital mobile radio towards future generation systems, final report," tech. rep., European Communities, EUR 18957, 1999.

Jun-Ki Hong received the B.S degree in system and computer engineering from Carleton University, Ottawa, Canada in 2010 and is currently pursuing the Ph.D. degree in electrical and electronics engineering at Yonsei University, Seoul, Korea. His main research interests are in the area of massive MIMO systems, antenna location optimization, and cooperative communications systems.

Han-Shin Jo is an Assistant Professor with the Department of Electronics and Control Engineering, Hanbat National University in Korea. He was a Postdoctoral Research Fellow in Wireless Networking and Communications Group, the Department of Electrical and Computer Engineering, the University of Texas at Austin from 2009-11. Dr. Jo developed LTE systems in Samsung Eletronics in 2011-12. He received the B.S., M.S., and Ph.D. degrees in Electrical and Electronics Engineering from Yonsei University Seoul, Korea, in 2001, 2004, and 2009, respectively. He received 2011 ETRI Journal Award. His research interests include Small cells, Heterogeneous network, Wireless ad-hoc network, Stochastic geometry, and Wireless broadband transmission.

Cheol Mun received the B.S., M.S., and Ph.D. degrees in electronics engineering from Yonsei University, Seoul, Korea, in 1995, 1997, and 2001 respectively. From March 2001 to February 2002, he joined Samsung Electronics Ltd., Suwon, Korea, as a Research Engineer. Currently, he is an Associate Professor at Department of Information and Communications Engineering, Korea National University of Transportation. His main research interests include the design and analysis of communication systems, such as MIMO and cooperative communications systems.

Jong-Gwan Yook (S'89-M'97-SM'12) was born in Seoul, Korea. He received the B.S. and M.S. degrees in electronics engineering from Yonsei University, Seoul, Korea, in 1987 and 1989, respectively, and the Ph.D. degree from The University of Michigan, Ann Arbor, MI, in 1996. He is currently a Professor with the School of Electrical and Electronic Engineering, Yonsei University. His main research interests are in the areas of theoretical/numerical EM modeling and characterization of microwave/millimeter-wave circuits and components, design of radio frequency integrated circuits (RFIC) and monolithic microwave integrated-circuit (MMIC), and analysis and optimization of high-frequency high-speed interconnects, including signal/power integrity (EMI/EMC), based on frequency as well as time-domain full-wave methods. Recently, his research team is developing various biosensors, such as carbon nano-tube RF biosensor for nanometer size antigen-antibody detection as well as remote wireless vital signal monitoring sensors.